OPEN SODIUM CHANNEL PROPERTIES OF SINGLE CANINE CARDIAC PURKINJE CELLS

M. F. SHEETS, B. E. SCANLEY, D. A. HANCK, J. C. MAKIELSKI, AND H. A. FOZZARD
The Cardiac Electrophysiology Labs, Departments of Medicine and the Pharmacological and Physiological Sciences, The University of Chicago, Chicago, Illinois 60637

ABSTRACT Open channel properties of canine cardiac Purkinje cell Na^+ channels were studied with single channel cell-attached recording and with whole cell macroscopic current recording in internally perfused cells. Single channel currents and membrane currents increased with an increase in Na^+ concentration, but showed evidence of saturation. Assuming first-order binding, the K_m for Na^+ was 370 mM. P_{Cs}/P_{Na} was 0.020 and P_K/P_{Na} was 0.094. The current–voltage relationship for single channels showed prominent flattening in the hyperpolarizing direction. This flattening was accentuated by 10 mM Ca^{2+} and was greatly reduced in 0 mM Ca^{2+}, indicating that the rectification was a consequence of Ca^{2+} block of the Na^+ channels. A similar instantaneous current–voltage relationship was seen for the whole cell membrane currents. These results demonstrate that the cardiac channel shows substantial Ca^{2+} block, although it is relatively insensitive to tetrodotoxin. The Na^+ and Ca^{2+} binding properties could be modeled by the four-barrier Eyring rate theory model, with similar values to those reported for the neuroblastoma Na^+ channel (Yamamoto, D., J. Z. Yeh, and T. Narahashi, 1984, *Biophys. J.*, 45:337–344).

INTRODUCTION

Passage of ions through membrane channels has often been treated as free electrodiffusion, described by the Goldman–Hodgkin–Katz equation (Hodgkin and Katz, 1949), in contrast to carrier-mediated transport of ions, which is considered to be a sequence of chemical reactions. However, in the past two decades evidence has accumulated that indicates ions interact with channels during their passage. For example, early experiments with intracellularly perfused squid axons demonstrated that outward currents through the Na^+ channel deviate from those predicted by the electrodiffusion equation (Chandler and Meves, 1965). Subsequently, Hille (1975) demonstrated saturable behavior of the Na^+ channel in frog nerve, and Begenisich and Cahalan (1980*a*, *b*) characterized saturation in squid axon. In addition, the instantaneous Na^+ current–voltage (IIV) relationship was shown to be nonlinear at negative membrane potentials (Chandler and Meves, 1965; Salgado and Narahashi, 1983; Stimers et al., 1985). Evidence suggesting that this nonlinearity is the result of divalent ion block of the Na^+ channel was reported by Taylor et al. (1976).

The availability of single Na^+ channel recordings makes possible a more detailed study of the interaction of Na^+ and Ca^{2+} with the Na^+ channel, and offers a means to characterize the behavior of Na^+ channels from different tissues. In neuroblastoma cells Yamamoto et al. (1984) demonstrated saturation and Ca^{2+} block of single Na^+ channels. Recently, Worley et al. (1986) found that tetramethyloxonium (TMO) treatment of rat brain Na^+ channels incorporated in planar lipid bilayers abolished this Ca^{2+} block and simultaneously reduced sensitivity of the channel to tetrodotoxin (TTX). The cardiac Na^+ channel is relatively insensitive to TTX (Brown et al., 1981), and this raises the question if it is also insensitive to Ca^{2+} block. While Ca^{2+} is known to affect cardiac excitability (Weidmann, 1955), this could be simply the result of divalent ion shielding of surface charge. Other important reasons to study the open channel properties of the cardiac Na^+ channel include the different sensitivity to local anesthetics and other antiarrhythmic drugs and the probable difference between the molecular structure of the cardiac Na^+ channel and neural Na^+ channel (Noda et al., 1986).

We have studied the open channel properties of the Na^+ channel of the cardiac Purkinje cell using both single channel measurements in intact cells and macroscopic membrane currents in intracellularly perfused cells. We demonstrate Na^+ saturation similar to that found in the neuroblastoma cell. Divalent ion block of the cardiac Na^+ current and of single Na^+ channels is prominent, despite relative TTX insensitivity. These interactions of Na^+ and Ca^{2+} with the channel can be modeled using the four-barrier Eyring rate theory model, yielding similar values for well depth and membrane potential effects to those of the nerve Na^+ channel. The divalent ion block satisfactorily explains the nonlinear IIV and current–voltage (i/V) relationships that have been seen respectively in membrane and single channel studies of cardiac cells (Cachelin et al.,

Address correspondence to Dr. Michael F. Sheets Box 440, University of Chicago Hospitals, 5841 S. Maryland Ave., Chicago, IL 60637.

1983; Kunze et al., 1985; Patlak and Ortiz, 1985). Despite the differences between cardiac and nerve Na^+ channel interaction with drugs and toxins, their open channel properties are similar. This Ca^{2+} block is sufficient to play a role in cardiac excitability. Some of these data were presented in abstract form (Hanck et al., 1986).

METHODS

Cell Preparation

The method for preparing single canine cardiac Purkinje cells has been described in detail elsewhere (Sheets et al., 1983). Briefly, canine Purkinje fibers from the hearts of adult mongrel dogs were cut into short segments (2–3 mm) and placed in Eagle's minimal essential medium modified to contain 0.1 mM free Ca^{2+} (by the addition of EGTA), 5.6 mM Mg^{2+}, 5.0 mM HEPES, 1 mg/ml albumin, and 5 mg/ml Worthington type I collagenase buffered to pH 6.2. The fibers were incubated in this digestion solution at 37°C, gassed with 100% O_2, and gently agitated in a water bath shaker for 3–4 h. After 15 min in 130 mM K-glutamate, 5.7 mM Mg^{2+}, 0.1 mM EGTA, 5.0 mM glucose, and 5.0 mM HEPES (pH 6.2), the cells were mechanically dispersed and maintained in Eagle's minimal essential medium with 1.0 mg/ml albumin and 5.0 mM HEPES (pH 7.2) at room temperature. They were studied within 12 h of isolation.

Patch Clamp Studies

Patch pipettes were made according to the method of Hamill et al. (1981). They were drawn in two stages using 1.5-mm outer diam, fiber-filled borosilicate glass capillary tubes (model 1B150F; World Precision Instruments, Inc., New Haven, CT). Tips were heat polished to an inside diameter of ~1 μm, and resistances when filled with isotonic salt solution were ~5 Mohm. The tapered end of the pipettes was coated with Sylgard 184 resin (Dow Corning Corp., Midland, MI) to reduce capacitance and electrical noise. The pipettes were usually filled with a solution of 140 mM NaCl, 5.4 mM KCl, 1.8 mM $CaCl_2$, 1 mM $MgCl_2$, and 10 mM HEPES buffer at pH 7.4. In some experiments the Ca^{2+} was omitted or increased to 10 mM, while in other experiments the NaCl was increased to 280 mM.

Freshly prepared single canine Purkinje cells were placed in a bath solution containing 150 mM KCl, 1 mM $MgCl_2$, 10 mM HEPES (pH 7.4), and 10 mM glucose at a temperature of 10°–13°C. The pipette was advanced until the cell membrane barely dimpled, where it sealed after gentle suction. All studies were on cell-attached patches containing four or fewer channels to reduce overlap of channel currents and in which seal resistances were stable. The number of Na^+ channels in each patch was determined by examination of the records for overlapping currents, and confirmed by a maximum likelihood calculation based on the method of Patlak and Horn (1982).

Single channel recordings were made with a Dagan 8900 patch clamp/whole cell clamp. The head stage was constructed according to a custom design (J. Rae and R. Levis, Rush Medical College, Chicago, IL). The signal was filtered at 2 KHz with an 8-pole Bessel filter (Frequency Devices, Inc.). A capacity compensation circuit was used to minimize the capacity transient, and further correction was performed during analysis by the subtraction of averaged sweeps without openings. Experimental protocols were controlled by an IBM-PC with a TM-100 D/A converter (Tekmar Co., Cincinnati, OH). The membrane patch was depolarized repetitively at 1 Hz to test potentials for 45 ms, from a holding potential that was usually −120 to −140 mV (assuming a resting membrane potential of 0 mV). Data were acquired at 10 KHz and were stored directly on floppy disk. Average single currents were derived from histograms of the set of all sampled current values during the test step, yielding plots like that in Fig. 1. The peak centered at zero is the baseline noise, and the peaks to the right are the open channel current distributions. Mean channel open time was obtained from histograms of open durations fitted by a single exponential using a least squares method. The first 0.5 ms was discarded for these fits because the frequency response of the recording system prevented accurate measurement of these very short openings. The open durations were measured as the time above half-amplitude currents (Sachs et al., 1982).

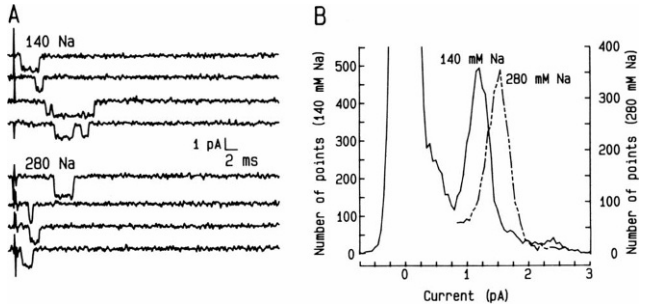

FIGURE 1 (*A*) Four consecutive sweeps showing single Na^+ channel currents in a Purkinje cell attached patch with 140 mM (*top*) and 280 mM (*bottom*) Na^+ in the patch pipette. (*B*) Amplitude histogram of single channel currents at test potential −50 mV with either 140 mM (*solid line*) or 280 mM (*broken line*) Na^+ in the patch pipette. The superimposed amplitude histograms were adjusted to have the same height by use of different scales.

Perfused Cell Experiments

All experiments were performed with single canine cardiac Purkinje cells prepared as above. A single glass suction pipette with a large pore of ~25-μm diam was used for both voltage clamp and internal perfusion as described in Makielski et al. (1987). In brief, a single cell with normal striation pattern, no membrane blebs, and a similar diameter as the pipette aperture was selected. The cell was drawn into the aperture until about one-third remained outside of the pipette (range for cell capacitance was 40–90 pF). The cell was allowed to seal to the aperture walls, then the segment of the cell within the pipette was ruptured by a manipulator-controlled wire, to allow free access of the pipette solution to the cell interior. The response time of the voltage clamp circuitry provided step changes that settled to within 1% of the final potential by 10 μs, while the membrane capacity time constant, τ_{cap}, with R_s compensation was usually <5 μs and series resistance was usually <3 ohm-cm^2 (Makielski et al., 1987). Currents recorded from these segments of membrane will be identified as "membrane currents" (I_{Na}), to distinguish them from single channel currents (i_{Na}).

Command voltage steps were generated by a 12-bit D/A converter and currents were recorded by a 12-bit A/D converter (Masscomp 5500 System microcomputer, Wesford, MA). For peak current voltage (I-V) relationships, current responses to step depolarizations were digitized at 10 μs per point, digitally filtered (Gaussian) at 5 KHz, and peak I_{Na} calculated by subtracting the leak current at the end of the 25-ms step depolarization from the peak transient current. Capacity subtraction was not performed because the short τ_{cap} allowed for clear separation of I_{Na} from I_{cap} (differences between measurements with and without subtraction were less than 1 nA).

For instantaneous current voltage experiments, current responses were digitized at 3.33 μs per point, leak corrected (assuming a linear leak, see Makielski et al., 1987) and capacitance corrected (using an average capacity transient constructed from hyperpolarizing and depolarizing voltage steps that did not activate I_{Na} and that were unlikely to elicit gating current). The current measurement was then made by averaging four points beginning at 40 μs after the test clamp step (see Stimers et al., 1985 and Yamamoto et al., 1985). All voltage protocols had a cycle frequency of 0.4 Hz.

External solution changes were made within 30 s by moving the cell

from the inlet of one bath chamber to the inlet of another bath chamber separated by a 10-mm length of plexiglass. For internal solution changes, a four way mechanical valve controlled the internal solution just proximal to the inlet of the suction pipette and internal solution changes were usually accomplished in less than 2 min. Solution changes were determined to be complete when the experimental reversal potential was the same as the predicted reversal potential (using the Nernst equation) and the current response to a step depolarization stabilized.

Table I shows the solutions (in millimolar) for the experiments in which Na^+ concentration was varied. The pH was 7.15 adjusted with CsOH. All experiments were done at 12°–16°C.

The extracellular solution for determination of the relative permeability of Cs^+ and Na^+ contained (mM) 15 NaCl, 134 Tris-Cl, 3.0 $CaCl_2$, 1.0 $MgCl_2$, 5.5 glucose, and 10 HEPES (pH 7.2), while intracellular solution contained 134 CsF, 15 Tris-F, 5 EGTA, 5.5 glucose, and 10 HEPES (pH 7.2).

Solutions to study the effect on I_{Na} kinetics by external Cs^+ were the following (mM): intracellular solution contained 149 Na^+, 15 H_2PO_4, 100 F^-, 10 EGTA, 5.5 glucose, and 10 HEPES (pH 7.2 adjusted by NaOH); extracellular solution contained either 149 KCl or 149 CsCl and with 1.0 $MgCl_2$, 3.0 $CaCl_2$, 5.5 glucose, and 10 HEPES (pH 7.2). For study of the effect of internal Cs^+ on I_{Na} kinetics the solutions were (mM): intracellular solution contained either 104 CsF, 45 NaF, 10 EGTA, and 10 HEPES (pH 7.2) or 113 KF, 36 NaF, 10 EGTA, and 10 HEPES (pH 7.2); extracellular solution contained 45 NaCl, 104 CsCl, 2 $CaCl_2$, and 10 HEPES (pH 7.2).

For experiments examining the effects of extracellular Ca^{2+}, the internal solution was intracellular solution D (Table I), while the external solution was extracellular solution B, but with Ca^{2+} either 3.0 or 10 mM.

Junction potentials between the internal and external solutions were corrected by the method of Oxford (1981). Briefly the junction potential required to null the current across the circuit of Ag-AgCl pellet/3.0 M KCl agar bridge/internal solution/3.0 M KCl agar bridge/external solution/3.0 M KCl agar bridge/Ag-AgCl pellet was subtracted from the command potential. For solutions when the major cations were either Cs^+ or Na^+, the junction potential was less than 0.6 mV and was therefore neglected.

Data Analysis

Calculations for the prediction of current assuming ionic independence used Eq. 1 (Hille, 1984). Relative P_{Cs} and P_K were measured by experimentally determining the reversal potential from peak I-V relationships or from instantaneous current voltage plots and from Eq. 2.

$$\frac{I'_{Na}}{I_{Na}} = \frac{[Na]'_i - [Na]'_o \exp(EF/RT)}{[Na]_i - [Na]_o \exp(EF/RT)}, \quad (1)$$

where E is membrane potential and F, R, and T have their usual meanings.

$$E_{rev} = RT/F \ln P_{Na}[Na]/P_x[X], \quad (2)$$

where [X] is [Cs] or [K]. Concentrations and not activities were used for these calculations since the activity coefficients of Na^+ and Cs^+ are nearly identical (Robinson and Stokes, 1959) and the ionic strength remained constant between the solution changes.

Mathematical models were programmed in the "C" programming language on an IBM-AT computer using the simulation control program (SCOP) from the National Biomedical Simulation Resource (Duke University, Durham, NC).

RESULTS

Current Responses to Change in Na^+ Concentration

Single Channel Experiments. Investigation of current responses to changes in extracellular Na^+ (Na_o) were studied by measuring single channel currents in cell-attached patches with either 140 mM or 280 mM Na_o (Fig. 1 *A*). In both cases 1.8 mM Ca^{2+} and 1.0 mM Mg^{2+} were in the patch pipettes. The experiments were performed at 10°–13°C to delay channel openings and prolong channel open times. The bath solution contained 150 mM K^+ to maintain the cell's resting potential close to 0 mV, and low Ca^{2+} to eliminate contractions. The average single channel current at each potential was measured from amplitude histograms. As illustrated in Fig. 1 *B* for steps to −50 mV, the increase in amplitude of the single channel current with 280 mM Na_o was modest but definite.

Plots of the current voltage (i/V) relationships are shown in Fig. 2 where each point represents the average of currents from 70 to 420 single openings at the voltage indicated. Even though Na_o was doubled, the single channel current increased by only ~50%, and not by the ~90% expected from Eq. 1 (using activities instead of concentrations). Note that i/V relationships were nonlinear and became flatter in the more negative voltage range. Single channel conductance in 140 mM Na_o, estimated from the

TABLE I
SOLUTIONS FOR INDEPENDENCE STUDIES IN PERFUSED CELL EXPERIMENTS

	Extracellular solutions (mM)						
	Na	Cs	Ca	Mg	Cl	Glucose	HEPES
A	15	134	3.0	1.0	157	5.5	10
B	45	104	3.0	1.0	157	5.5	10
C	120	29	3.0	1.0	157	5.5	10

	Intracellular solutions (mM)								
	Na	Cs	EGTA	F	H_2PO_4	Glucose	HEPES	Mg-ATP	8,Br-cAMP
D	15	134	5.0	134	15	5.5	10	0.1	0.1
E	45	104	5.0	134	15	5.5	10	0.1	0.1
F	120	29	5.0	134	15	5.5	10	0.1	0.1

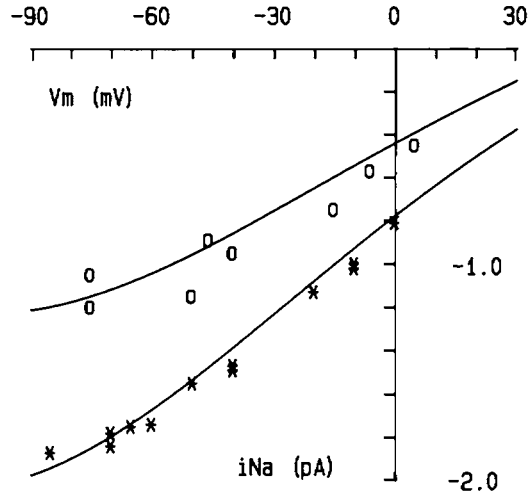

FIGURE 2 Plots of the i/V relationships with 140 mM (0) or 280 mM (×) in the patch pipette. Each point represents the average of 70–420 single channel openings. The solid lines are the model predictions using the parameters from Fig. 9.

steeper part of the i/V relationship, was 12 pS. It is not possible to be sure of the reversal potential from the single channel measurements, since the i/V relationship appeared to be nonlinear as it approached the zero current point. Linear extrapolation yielded a value of +50 mV, which is close to the E_{Na} of +55 mV, calculated from Nernst equation assuming 140 mM K_i, 0 mM Na_i and P_K/P_{Na} of 0.094 (see below). The i/V relationship in 280 mM Na^+ and 1.8 mM Ca^{2+} extrapolated to a somewhat more positive reversal potential. The approximate single channel conductance in 280 mM Na_o, based on the steepest slope of the i/V relationship, was 17 pS. Mean open times in 140 mM and 280 mM Na_o both averaged 1.1 ms at −40 mV and were 0.80 ms and 0.85 ms, respectively, at −10 mV.

Over the entire voltage range studied, the increase in single channel current with 280 mM Na^+ is less than that predicted from ionic independence. The binding constant (K_m) for Na^+ at 0 mV was estimated to be 370 mM using a ratio of the single channel currents obtained in 140 mM and 280 mM Na_o and Eq. 3, which assumes Na^+ binding to be a first order process. However, saturation of the Na^+ channel by Na^+ does not fully explain the nonlinear i/V relationship. As discussed below, the nonlinearity probably results from interference of the Na^+ current by divalent cations.

$$i = i_{max}Na_o/(K_m + Na_o). \quad (3)$$

Perfused Cell Experiments. Current responses to different Na^+ gradients were also studied in voltage clamped single Purkinje cells. After changing Na_o or Na_i, peak I_{Na} was measured in response to a 25-ms test depolarization from a holding potential of −150 mV and compared with the predicted peak current assuming ionic independence.

Fig. 3 shows the results in two cells for changes in Na_o while maintaining Na_i constant. Na_o was either 15, 45, or 120 mM with Na_i being 15 mM. After correction for Cs^+ permeability, effective Na_o was 18, 47, or 121 mM and Na_i was 18 mM (see below). At test voltages of −30 and −10 mV, peak I_{Na} measured with 45 or 120 mM Na_o was normalized to I_{Na} with 15 mM Na_o. Experiments in 15 mM Na_o were the last to be performed to eliminate the possibility of current rundown as the cause of the normalized currents being smaller than predicted by ionic independence. As illustrated in Fig. 4, the increase in the measured peak I_{Na} was less than predicted from ionic independence for both 45 and 120 mM Na_o.

Then Na_o was maintained constant at 15 mM and Na_i changed to 15, 45, or 120 mM (after correction for Cs permeability Na_o = 18, Na_i = 18, 47, 121, respectively). The results for three cells at test voltages of +10 and +40 mV are shown in Fig. 4 with the currents normalized to those obtained with 15 mM Na_i. Again the increase in the peak I_{Na} is less than that predicted by ionic independence.

It is necessary to consider the possible effects of the Na^+ substitute cation, Cs^+, on Na^+ currents. Cs^+ was chosen as the substitute cation for the following reasons: the activity coefficient of Cs^+ and Na^+ are similar; Cs^+ has a relatively high ionic conductance, thus minimizing R_s; Cs^+ appears not to affect sodium channel kinetics (see below); Cs^+ blocks K^+ currents; and Cs^+ has a low Na^+ channel permeability. Since Cs^+ does have a finite permeability through Na^+ channels, its permeability must be included in the calculations for the prediction of I_{Na} assuming ionic independence. In a separate set of experiments, with the internal solution containing 134 mM Cs^+ and the external solution containing 15 mM Na^+, the P_{Cs}/P_{Na} was calculated from E_{rev} to be 0.020 (n = 3, range 0.019–0.021). The contribution of Cs^+ permeability to the total ionic current through Na^+ channels was included in the prediction of peak current assuming ionic independence by multiplying 0.020 by [Cs^+] and adding the product to actual [Na^+] thus obtaining the effective [Na^+]. Although cation permeability ratios may vary with permeant ion concentration

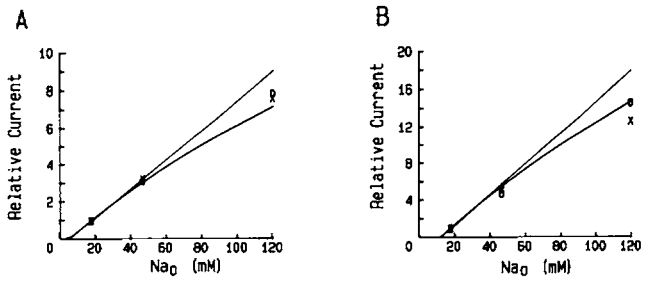

FIGURE 3 Normalized peak I_{Na} of two perfused single Purkinje cells (0, ×) as a function of extracellular permeant ion concentrations of 18, 47, and 121 mM at test potentials of −30 mV (*A*) and −10 mV (*B*). The straight lines represent normalized current predicted by ionic independence while the curved lines represent model fits to the data (see text).

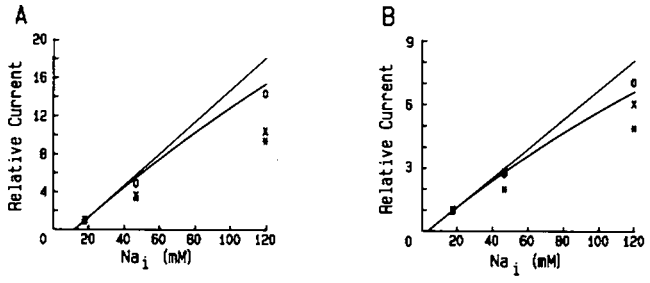

FIGURE 4 Normalized peak I_{Na} of three perfused single Purkinje cells (0, ×, *) as a function of intracellular permeant ion concentrations of 18, 47, and 121 mM at test potentials of +10 mV (*A*) and +40 mV (*B*). The straight lines represent normalized current predicted by ionic independence while the curved lines represent model fits to the data (see text).

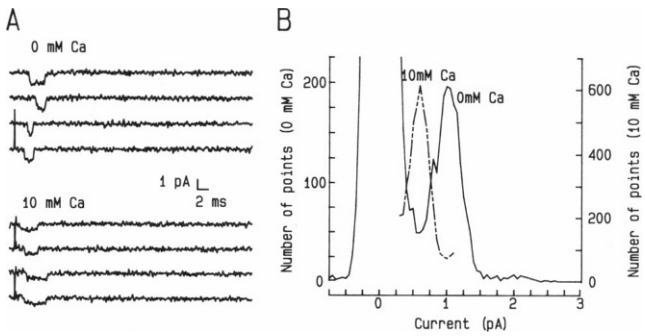

FIGURE 5 (*A*) Four consecutive sweeps showing single Na^+ channel currents of a Purkinje cell attached patch with 1.0 mM Mg^{2+} and either 0 mM (*top*) or 10 mM (*bottom*) Ca^{2+} in the patch pipette. (*B*) Amplitude histogram of single channel currents at test potential −40 mV with either 0 mM (*solid line*) or 10 mM (*broken line*) Ca^{2+} in the patch pipette. The number of events in 10 mM Ca^{2+} were scaled so that its peak would be the same as that in 0 mM Ca^{2+}.

(Cahalan and Begenisich, 1976), the effect of any such variation of P_{Cs} would be small, since $[Na^+]$ is increasing as $[Cs^+]$ is decreasing. Also, Cs^+ block as a cause of I_{Na} saturation is excluded because as $[Na^+]$ increases and $[Cs^+]$ decreases, Na^+ channel block should decrease and allow for a greater I_{Na}, the opposite of our results.

Oxford and Yeh (1985) showed in squid that as $[Na^+]_i$ increased and $[Cs^+]_i$ decreased I_{Na} inactivation slowed. It is unlikely that internal Na/Cs substitution affected I_{Na} kinetics in this way to cause our experimental results because this effect would give results favoring ionic independence, the opposite of our results. To investigate the effect of Cs_i on Na^+ current kinetics, we compared the current responses from step depolarizations to positive potentials in a cell perfused externally with 45 mM Na^+ and 104 mM Cs^+ and perfused internally with 104 mM Cs^+ and 45 mM Na^+ or 113 mM K^+ and 36 mM Na^+. The time courses of outward currents were identical. Similarly, to investigate the effect of Cs_o on the kinetics of the Na^+ current, we compared the current responses from step depolarizations in a cell perfused internally with 149 mM Na^+ and externally with 150 mM K^+ or 150 mM Cs^+. At step potentials positive to +40 mV, where the outward current was almost completely carried by Na^+ ions, currents were identical. Unless both K^+ and Cs^+ alter I_{Na} kinetics identically, it is unlikely that Na/Cs substitution internally or externally had a significant effect.

From the above experiments, the E_{rev} for 149 mM Na_i and 150 mM K_o was −58 mV (n = 2 cells) and the calculated relative P_K/P_{Na} was 0.094.

Effects of Extracellular Ca^{2+}

Single Channel Recordings. Single channel recordings were made with the pipette containing 140 mM Na^+, 1.0 mM Mg^{2+} and either 0 mM ($<10^{-5}$) or 10 mM Ca^{2+}. Examples of the single channel recordings are shown in Fig. 5 *A*. Open channel noise did not appear to be greater in 10 mM Ca^{2+}. However, if the lower amplitude currents resulted from a rapid transient block of the channel by Ca^{2+}, this would be impossible to resolve because of the necessity to filter the signal at 2 KHz. Because channel currents in 10 mM Ca^{2+} were of much lower amplitude, longer duration openings were selected for the figure for them to be seen more easily. Mean open times were similar in the 0 and 10 mM Ca^{2+} solutions for steps to −40 mV (1.09 and 1.06 ms, respectively). However, mean open time in these cells was less near threshold potential. At −70 mV the mean open time in 10 mM Ca^{2+} was shorter than that in 0 mM Ca^{2+}, presumably as a consequence of a voltage shift produced by alteration of fixed negative surface charge. There is no reason to expect that the shorter open times in high Ca_o at hyperpolarized potentials affected the measurement of mean current amplitude, since the amplitude histograms remained nearly symmetrical, as judged from best-fit Gaussian distributions.

The single channel current amplitudes at −40 mV for the two solutions are illustrated in Fig. 5 *B*. The two histograms have different numbers of sample points at the single channel level, so for comparison they have been plotted to have the same peak height. Note that the width of the two peaks is about the same, supporting the impression that open channel noise was not increased in 10 mM Ca^{2+}. The i/V plots in different Ca_o are shown in Fig. 6. The single channel currents obtained in 10 mM Ca_o are less than those in 0 mM Ca_o, with the magnitude of the difference being voltage dependent. Even in 0 mM Ca_o the i/V relationship is slightly nonlinear although this probably represents block by the 1.0 mM Mg^{2+} that was also in the patch pipette solution (see model below).

Perfused Cell Experiments. The instantaneous current voltage relation was studied with either 3.0 or 10 mM Ca_o. I_{Na} was elicited with a conditioning step depolarization of 0 mV from a holding potential of −150 mV, and a test step was made 500 μs (in some experiments, 400 μs) after the conditioning step, over a range of potentials from

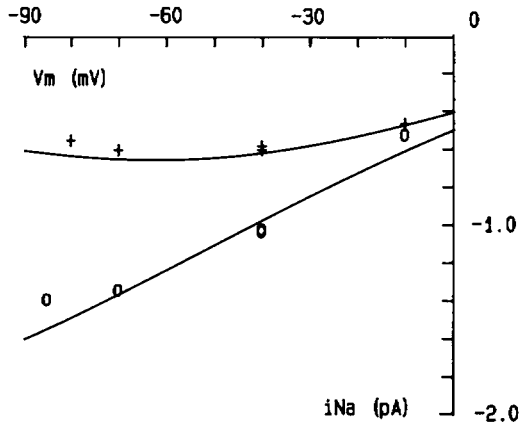

FIGURE 6 Plots of the i/V relationships with 1.0 mM Mg^{2+} and 0 mM (0) or 10 mM (*) Ca^{2+} in the patch pipette. Each point represents the average amplitudes of 34–240 single channel openings. The solid lines are model fits to the data (see text).

+80 mV to −120 mV, in 10 mV increments. Fig. 7 shows the first 100 μs of capacitance and leak corrected current traces from the onset of the test step. By 20 μs the current reached a maximum before the current declined. For test potentials more negative than −120 mV the I_{Na} did not achieve a plateau (decay was very rapid), and therefore these were not included.

Fig. 8 illustrates the IIV relationship in a Purkinje cell bathed in extracellular solutions containing 3 mM, then 10 mM Ca_o and then 3 mM Ca_o. The relationship in 3 mM Ca_o appears linear for test potentials positive to −40 mV except at +80 mV where rectification occurs due to asymmetrical Na^+ concentrations. However, at potentials negative to −70 mV the measured currents are less than predicted by a constant conductance. When Ca_o is increased to 10 mM, the deviation from a constant conductance is substantially increased and is consistent with Ca^{2+}

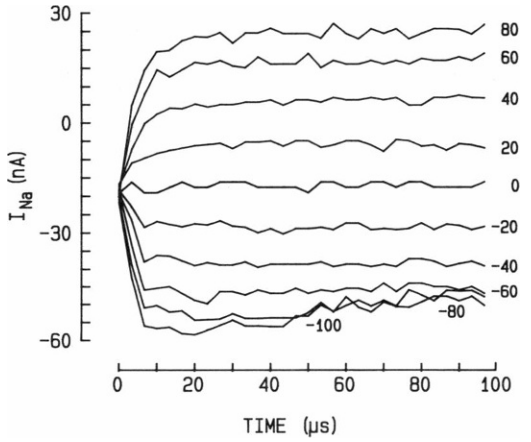

FIGURE 7 The first 100 μs of leak and capacitance corrected I_{Na} from an IIV protocol in a perfused Purkinje cell. I_{Na} was elicited during a step to test potentials from +80 to −100 mV in 10 mV increments after a 500-μs conditioning step to 0 mV. I_{Na} was measured at 40 μs after stepping to the test potential.

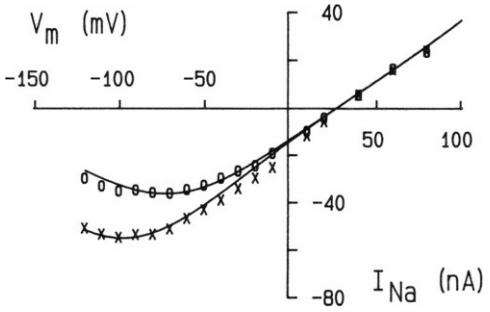

FIGURE 8 Instantaneous current voltage plot in a perfused Purkinje cell with either 3.0 mM (×) or 10.0 mM (0) Ca^{2+}. The lines represent model fits to the data (see text).

block of Na^+ current. However, the magnitude of the Ca^{2+} induced decrease of the Na^+ current appears less than that with the patch clamp experiments. The cause for the difference may be the difference in frequency response between the patch clamp and whole cell clamp (2 KHz vs. 100 KHz), the different voltage clamp protocols between the two voltage clamp methods or a more pronouced shift in the Na^+ current kinetics in the perfused cell experiments.

Although we attempted to study the effects of 0.6 mM Ca_o externally on IIV currents, it was difficult because of an increase in the holding current that occurred presumably from loss of the high resistance seal between the pipette and cell. However, from limited data with 0.6 mM Ca_o the IIV showed less deviation from linearity than the currents obtained in 3.0 mM Ca_o.

Comparison of Experimental Results with Predictions of a Four Barrier Model of the Na^+ Channel

To further our understanding of non-independence of I_{Na} and to help compare our findings with the Na^+ channel of nerve, we modeled the Na^+ channel as a series of energy barriers and wells with rate constants for individual transitions given by Eyring rate theory (Glasstone et al., 1941). A four-barrier three-well single occupancy model for the Na^+ channel (Hille, 1975) was used to fit both Ca^{2+} block and Na^+ saturation in the single channel studies and the membrane current studies. A three-barrier two-well model of the Na^+ channel allowing multiply occupied sites was used by Begenisich and Cahalan (1980*a*) to explain some additional channel characteristics, however we used the four-barrier model to allow direct comparison with recent measurements of Ca^{2+} block and Na^+ saturation in single neuroblastoma Na^+ channels (Yamamoto et al., 1984).

Rate constants for transitions of ions over barriers were calculated as described by Hille (1975), and the system of equations describing steady-state currents was solved using Gaussian elimination (Begenisich and Cahalan, 1980*a*). The model is appropriate only for open channel currents at

equilibrium and does not account for any changes in activation or inactivation kinetics that might be caused by monovalent or divalent cations. The model also assumes that the presence of divalent ions in the channel prohibits Na^+ ion passage and that the affinity of ion binding to the outer well is independent of other ions.

The parameters used for modeling our data are shown in Fig. 9 along with the Na^+ channel barrier and well values used by Hille (1975) in frog myelinated nerve and by Yamamoto et al. (1984) in neuroblastoma. For each ion there are 11 free parameters; three energy wells, four energy barriers, and four electrical distances (the proportion of the electrical field transversed between each energy well). The electrical distance and first well depth for Ca^{2+} were calculated directly from the data. The other parameters were assigned using values of previous studies as a starting point and changed to give the best fit to all of the data using the considerations discussed below. The depth

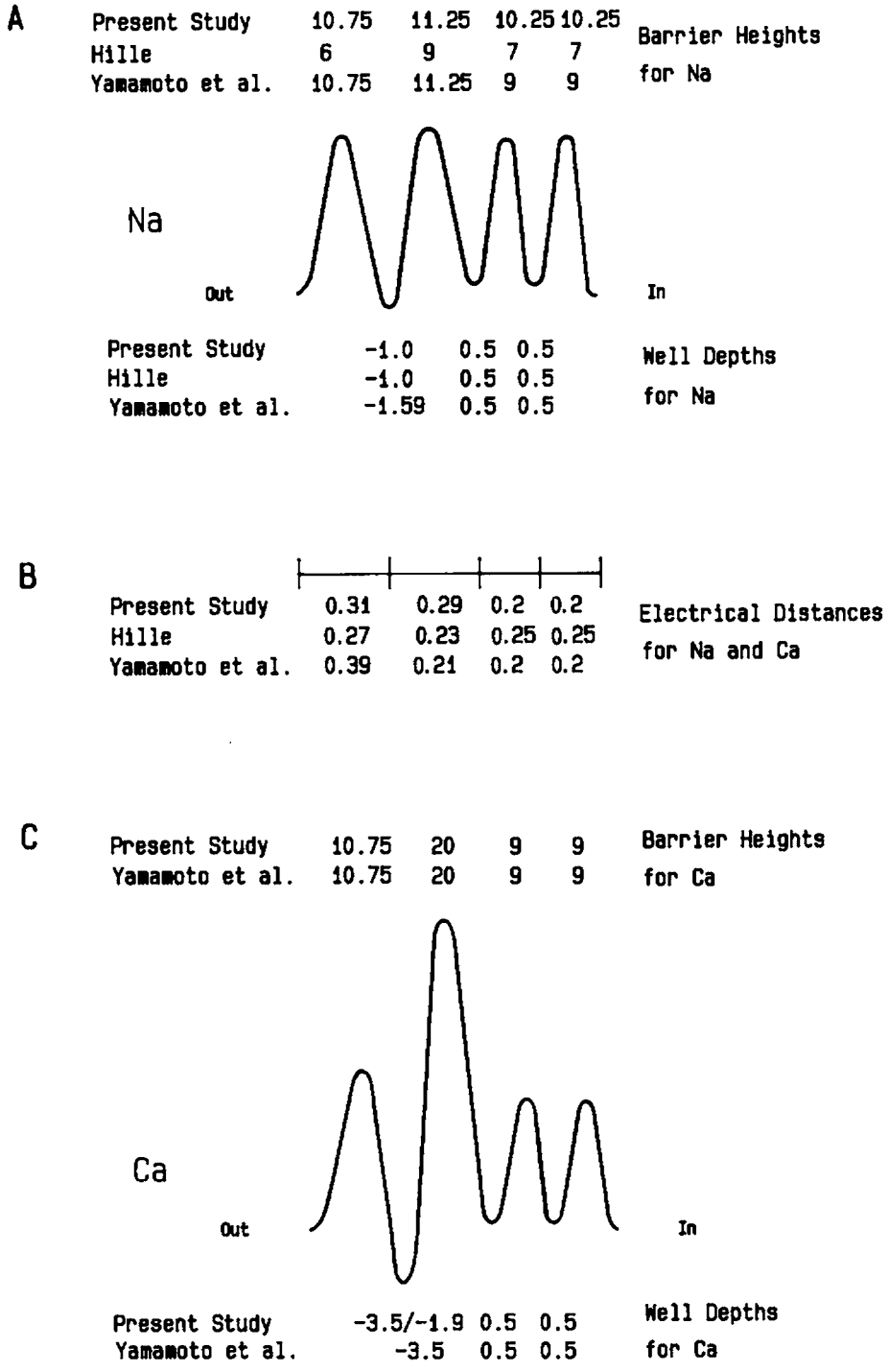

FIGURE 9 Schematic diagram of the four barrier, three well Erying rate theory model for Na^+ (*A*) and Ca^{2+} (*C*). For each ion, the barrier heights, listed above, and energy wells, listed below the schematic, are given in *RT* units. The electrical distances (*B*) are the same for Na^+ and Ca^{2+}. For comparison, the values for frog myelinated nerve (Hille, 1975) and neuroblastoma (Yamamoto et al., 1984) are shown for Na^+, and those for neuroblastoma are shown for Ca^{2+}. Note that two well depths are given for Ca^{2+} binding. -3.5 *RT* units applies to patch studies; -1.9 *RT* units applies to perfused cell studies.

of the outermost well (G2 in Fig. 9) for Ca^{2+} block was calculated by the method of Woodhull (1973). The binding constant (K_m)–voltage relation was determined by solving for K_m from Eq. 4 relating the current ratio (I_1/I_2) for the two Ca^{2+} concentrations used at each test potential.

$$I_1/I_2 = (Ca_2 + K_m)/(Ca_1 + K_m). \quad (4)$$

The K_m in the absence of an applied field ($K_m(0)$) was used to calculate the well depth using Eq. 5.

$$G2 = RT \ln K_m(0). \quad (5)$$

The electrical distance $D1$ is related to the slope (m) of the ln (Kd) – V relation by Eq. 6.

$$D1 = zF/mRT. \quad (6)$$

In the above equations R, T, and F have their usual meanings and z is the ionic charge.

$D1$ for Ca^{2+} binding was calculated from the IIV relations obtained in three cells at two divalent strengths and was found to be 0.31. All other electrical distances were assigned in a manner consistent with previous models. The same distances (adjusted for valence) were used for Na^+, although this must be regarded as only a reasonable assumption and not mandated by the data.

For Ca^{2+} the second barrier was chosen to be sufficiently high that there was negligible Ca^{2+} conductance through the Na^+ channel. The well depth for Ca^{2+} binding calculated from the aggregate patch clamp data was -3.5 RT units. The other model parameters for Ca^{2+} did not affect the fit to our data and were left identical to those of Yamamoto et al. (1984). Because we found the model fit to single channel current in 0 mM Ca_o improved by increasing the total divalent strength by 1.0 mM (due to the presence in the patch pipette solution of 1.0 mM Mg^{2+}), all model fits to the data used total divalent strength. Yamamoto et al. (1984) also described the effects of Mg^{2+} to be quantitatively similar to Ca^{2+}. The solid lines in Fig. 6 show the model has a close fit to the patch clamp currents in 0 and 10.0 mM Ca_o.

Use of the same model parameters, however, predicted more Ca^{2+} block at negative potentials than was seen in the perfused cell studies. Well depth for Ca^{2+} binding in the whole cell varied from -1.0 to -2.7 RT units in six experiments (three different cells at two divalent strengths). A straight line fit to the ln (Kd) – V relation for all of these experiments predicted a well depth of -1.9. The model fits to data from one cell is shown in Fig. 8 using a well depth of -2.3.

For Na^+, the outer two barrier heights used by Yamamoto et al. (1984) fit our single channel conductance well. However, it was necessary to increase the heights of the inner two barriers to allow I_{Na} rectification at potentials greater than 0 mV seen as a result of asymmetrical Na^+ concentrations in the perfused cell experiments. The inner and outer well depths could not be calculated from the perfused cell data because of the presence of significant Na^+ backflux. The outer well depth could be estimated from single channel studies because Na^+ backflux was negligible under experimental conditions. The first well depth was calculated to be -1.0 RT and is the same value used by Hille (1975). The inner two well depths for Na^+ were the values used in previous studies. The solid lines are drawn by the model for patch clamp data (Fig. 2) and perfused cell data (Figs. 3 and 4), and show that the model predicts the deviations from ionic independence observed experimentally.

DISCUSSION

Open channel properties of the cardiac Na^+ channel were studied with the complimentary experimental techniques of patch clamping of single Na^+ channels in intact cells and membrane currents in intracellularly perfused cells. The cardiac channel shows cation selectivity, Na^+ saturation, and Ca^{2+} block. Modeling this behavior with a four-barrier Eyring rate theory model shows good fit to the data, with a cation binding site about one-quarter to one-third the distance through the membrane field. Binding energies for Na^+ and Ca^{2+} are similar to those found by Yamamoto et al. (1984) for neuroblastoma Na^+ channels, suggesting that cardiac and nerve Na^+ channels have similar open channel behavior.

The agreement of open channel properties may be surprising for several reasons. The cardiac channel is thought to be a single molecule of 260-kD mass, with only partial homology with nerve channels, which also have two additional subunits (Noda et al., 1986). Second, the drug and toxin binding properties of the two channels are different (Catterall, 1980), including dramatic difference in sensitivity to TTX. Coupling between TTX sensitivity and open channel Ca^{2+} block in brain Na^+ channels was reported by Worley et al. (1986), who suggested that the two agents might act on the same site because they could reduce both effects by modification with TMO. However, we found cardiac channels, which are relatively TTX resistant, are sensitive to Ca^{2+} block, suggesting that the TTX site and the Ca^{2+} site may not be the same in cardiac Na^+ channels. Other reasons for doubting that the two sites are the same can also be cited. For example, Huang et al. (1979) have shown that a neuroblastoma cell line with TTX-resistant Na^+ channels shows the same proton blocking characteristic as TTX-sensitive Na^+ channels of another neuroblastoma cell line. In addition, the STX binding site does not appear to be inside the membrane field, while the Ca^{2+} binding site is within the field (Moczydlowski et al., 1984).

Ca^{2+} Block. The block of Na^+ current by Ca^{2+} was demonstrated in both the intracellularly perfused Purkinje cell and in the single channel recordings on intact cells. This block was strikingly voltage-dependent in both

studies, as was also shown by Yamamoto et al. (1984) and Worley et al. (1986) for nerve channels. Presumably this Ca^{2+} block was due to transitory occlusion of the channel by the divalent ion, producing flickering of the single channel current that could not be recorded accurately because of the frequency response limitations of the single channel recordings. Instead, the filtered signal gave the appearance of a lower single channel conductance. Whatever the molecular mechanism of the block, the four-barrier modeling parameters are nearly identical, suggesting that the Ca^{2+} block in cardiac channels is not different from that of nerve. As previously mentioned, Ca^{2+} block occurs even with relative Na^+ channel insensitivity to TTX in cardiac muscle.

Selectivity and Na^+ Saturation. We measured P_{Cs}/P_{Na} and P_K/P_{Na} from reversal potential experiments in the perfused cells and calculated the relative permeabilities to be 0.020 and 0.094, respectively. The relative K^+ permeability is similar to that of frog nerve (0.086; Hille, 1972), squid axon (0.083; Chandler and Meves, 1965), and *Myxicola* axon (0.076; Ebert and Goldman, 1976). The relative Cs^+ permeability is also similar to that of nerve (0.016 in squid, Chandler and Meves, 1965; <0.012 in frog nerve, Hille, 1972).

The K_m of 370 mM for Na^+ was derived only from the single channel measurements, but the model fit to the perfused cell data was good. This binding is sufficient to influence the interpretation of Na^+ currents during experimental changes in ion concentrations. The magnitude of the single channel conductance was also accurately predicted by the same second barrier height as was used by Yamamoto et al. (1984), emphasizing that the cardiac and nerve single channel conductances are not very different. It was necessary, however, to increase the two inner barrier heights to allow for rectification at potentials positive to 0 mV. The smaller barrier heights used by Hille (1975) for frog myelinated nerve produced an excessive single channel conductance.

The Model. The use of the four-barrier model made comparison of the cardiac Na^+ channel with the nerve channel easier, but the goodness of fit of the Na^+ and Ca^{2+} interactions with the channel does not mean that the model is necessarily correct. Other models may have fit equally well. The concept of an energy well at some point within the channel, where the ion interacts most closely with the channel protein, is essential to explain the experimental results. However, other factors of importance to the ion passing through the channel, such as convergence of ions into the channel mouth and field effect of nearby charges, are not explicitly represented in the model (Dani, 1986). With continued progress toward detailed structural understanding of the different Na^+ channel types, these functional studies will become more easily interpreted.

Role of Ca^{2+} Block in Cardiac Excitation. Extracellular Ca^{2+} has long been known to reduce excitability in nerve and muscle. This was clearly illustrated at the cellular level for cardiac cells by Weidmann (1955), who showed that larger $[Ca^{2+}]_o$ greatly increased the threshold current for excitation in sheep cardiac Purkinje fibers. Frankenhaeuser and Hodgkin (1957) suggested that the mechanism for this effect may be a shielding of fixed negative charges on the external surface of the membrane, which causes an increase in the electric field sensed by the channel voltage-sensitive gating system. This shielding phenomenon has been amply substantiated by a variety of experimental studies. We could also see an effect caused by this change in the field. Cardiac Na^+ channel mean open time is voltage sensitive in the threshold region, and changes in Ca^{2+} produced a shift that was consistent with the shielding effect. However, the direct block of single Na^+ channels is substantial and at threshold voltages, current is reduced by one-third to one-half. It seems likely that the change in excitability is a combination of a reduction in activation of Na^+ channels and a reduction in their mean open time, both resulting from shielding, and additionally a direct Ca^{2+} block, reducing single channel current.

This work was supported by grants PO1 HL-20692, K11 HL-01572, K11 01447, and GM-07281.

Received for publication 8 September 1986 and in final form 17 February 1987.

REFERENCES

Begenisich, T. B., and M. D. Cahalan. 1980*a*. Sodium channel permeation in squid axons. I: Reversal potential experiments. *J. Physiol. (Lond.)*. 307:217–242.

Begenisich, T. B., and M. D. Cahalan. 1980*b*. Sodium channel permeation in squid axons. II: Non-independence and current-voltage relations. *J. Physiol. (Lond.)*. 307:243–257.

Brown, A. M., K. S. Lee, and T. Powell. 1981. Voltage clamp and internal perfusion of single rat heart muscle cells. *J. Physiol. (Lond.)*. 318:455–477.

Cachelin, A. B., J. E. DePeyer, S. Kokubun, and H. Reuter. 1983. Sodium channels in cultured cardiac cells. *J. Physiol. (Lond.)*. 340:389–401.

Cahalan, M., and T. B. Begenisich. 1976. Sodium channel selectivity: dependence on internal permeant ion concentration. *J. Gen. Physiol.* 68:111–125.

Campbell, D. T., and B. Hille. 1976. Kinetic and pharmacological properties of the sodium channel of frog skeletal muscle. *J. Gen. Physiol.* 67:309–323.

Catterall, W. A. 1980. Neurotoxins that act on voltage-sensitive sodium channels in excitable membranes. *Annu. Rev. Pharmacol. Toxicol.* 20:15–43.

Chandler, W. K., and H. Meves. 1965. Voltage clamp experiments on internally perfused giant axons. *J. Physiol. (Lond.)*. 180:788–820.

Dani, J. A. 1986. Ion-channel entrances influence permeation. Net charge, size, shape, and binding considerations. *Biophys. J.* 49:607–618.

Ebert, G. A., and L. Goldman. 1976. The permeability of the sodium channel in Myxicola to the alkali cations. *J. Gen. Physiol.* 68:327–340.

Frankenhaeuser, B., and A. L. Hodgkin. 1957. The action of calcium on the electrical properties of squid axons. *J. Physiol. (Lond.).* 137:218–244.

Glasstone, S., K. J. Laidler, and H. Eyring. 1941. The Theory of Rate Processes. McGraw Hill Book Company, New York.

Hanck, D. A., M. F. Sheets, B. E. Scanley, J. C. Makielski, and H. A. Fozzard. 1986. Calcium dependence of single Na channel rectification and instantaneous IV relation in cardiac Purkinje cells. *Biophys. J.* 49(2, Pt. 2):347a. (Abstr.)

Hamill, O. P., A. Marty, E. Neher, B. Sakmann, and F. J. Sigworth. 1981. Improved patch clamp techniques for high-resolution current recording from cells and cell-free membrane patches. *Pfluegers Arch. Eur. J. Physiol.* 391:85–100.

Hille, B. 1972. The permeability of the sodium channel to metal cations in myelinated nerve. *J. Gen. Physiol.* 59:637–658.

Hille, B. 1975. Ionic selectivity, saturation, and block in sodium channels: a four-barrier model. *J. Gen. Physiol.* 66:535–560.

Hille, B. 1984. Ionic Channels of Excitable Membranes. Sinauer Associates, Inc. Sunderland, MA. 251 pp.

Hodgkin, A. L., and B. Katz. 1949. The effect of sodium ions on the electrical activity of the giant axon of the squid. *J. Physiol. (Lond.).* 108:37–77.

Huang, L. M., W. A. Catterall, and G. Ehrenstein. 1979. Comparison of ionic selectivity of batrachotoxin-activated channels with different tetrodotoxin dissociation constants. *J. Gen. Physiol.* 73:839–854.

Kunze, D. L., A. E. Lacerda, D. L. Wilson, and A. M. Brown. 1985. Cardiac Na currents and the inactivating, reopening, and waiting properties of single cardiac Na channels. *J. Gen. Physiol.* 86:691–719.

Makielski, J. C., M. F. Sheets, D. A. Hanck, C. T. January, and H. A. Fozzard. 1987. Sodium current in voltage clamped internally perfused cardiac Purkinje cells. *Biophys. J.* 52:1–11.

Moczydlowski, E., S. Hall, S. S. Garber, G. S. Strichartz, and C. Miller. 1984. Voltage dependent blockade of muscle Na^+ channels by guanidinium toxins. *J. Gen. Physiol.* 84:687–704.

Noda, M., T. Ikeda, T. Kayano, H. Suzuki, H. Takeshima, M. Kurasaki, H. Takahashi, and S. Numa. 1986. Existence of distinct sodium channel messenger RNAs in rat brain. *Nature (Lond.).* 320:188–192.

Oxford, G. S. 1981. Some kinetic and steady-stage properties of sodium channels after removal of inactivation. *J. Gen. Physiol.* 77:1–22.

Oxford, G. S., and J. Z. Yeh. 1985. Interactions of monovalent cations with sodium channels in squid axon. I. Modification of physiological inactivation gating. *J. Gen. Physiol.* 85:583–602.

Patlak, J. B., and R. Horn. 1982. Effect of N-bromoacetamide on single sodium channel currents in excised membrane patches. *J. Gen. Physiol.* 79:333–352.

Patlak, J. B., and M. Ortiz. 1985. Slow currents through single sodium channels of the adult rat heart. *J. Gen. Physiol.* 86:89–104.

Robinson, R. A., and R. H. Stokes. 1959. Electrolyte Solutions. Butterworth Co., London. 231–232.

Sachs, F., J. Neil, and N. Barkakati. 1982. The automated analysis of data from single ionic channels. *Pfluegers Arch. Eur. J. Physiol.* 395:331–340.

Salgado, V. L., and T. Narahashi. 1983. Current-voltage relations of normal and fenvalerate-modified sodium channels in crayfish axons. *Biophys. J.* 41(2, Pt. 2):51a. (Abstr.)

Sheets, M. F., C. T. January, and H. A. Fozzard. 1983. Isolation and characterization of single canine Purkinje cells. *Circ. Res.*53:544–548.

Spalding, B. C. 1980. Properties of toxin-resistant sodium channels produced by chemical modification in frog skeletal muscle. *J. Physiol. (Lond.).* 305:485–500.

Stimers, J. R., F. Bezanilla, and R. E. Taylor. 1985. Sodium channel activation in the squid giant axon. *J. Gen. Physiol.* 85:65–82.

Taylor, R. E., C. M. Armstrong, and F. Bezanilla. 1976. Block of sodium channels by external calcium ions. *Biophys. J.*16(2, Pt. 2):27a. (Abstr.)

Weidmann, S. 1955. Effects of calcium ions and local anaesthetics on electrical properties of Purkinje fibres. *J. Physiol. (Lond.).* 129:568–582.

Woodhull, A. N. 1973. Ionic blockage of sodium channels in nerve. *J. Gen. Physiol.* 61:687–708.

Worley, J. F., III, R. J. French, and B. K. Krueger, 1986. Trimethyloxonium modification of single batrachotoxin-activated sodium channels in planar bilayers. *J. Gen. Physiol.* 87:327–349.

Yamamoto, D., J. Z. Yeh, and T. Narahashi. 1984. Voltage-dependent calcium block of normal and tetramethrin-modified single sodium channels. *Biophys. J.*45:337–344.